Synthesis and characterization of Al-doped ZnO terrace-truncated nanocone structure by the advanced spray pyrolysis deposition technique

Synthesis and Characterization of Al Doped ZnO Terrace-Truncated Nanocone Structure by Advanced Spray Pyrolysis Deposition Technique.

Sameera Attanayake[1*], Masayuki Okuya[2], and Kenji Murakami[2]

[1]*Graduate School of Science and Technology, Shizuoka University, Hamamatsu 432-8011, Japan*

[2]*Graduate School of Integrated Science and Technology, Shizuoka University, Hamamatsu 432-8011, Japan*

**E-mail: a.m.s.l.b.attanayake@shizuoka.ac.jp*

Abstract

We have synthesized terrace-truncated nanocone structure of Al doped ZnO by using advanced spray pyrolysis deposition technique. In this study, we have proposed the growth mechanism of terrace-truncated nanocone structure. Average top diameter is 35-40 nm and the height of the structure vary in between 600-650 nm. The nanostructure was favored along the c-axis as confirmed by x-ray diffraction patterns. The electrical conductivity and optical transmittance in the visible range are 5.1×10^3 $\Omega^{-1}cm^{-1}$ and 80 % respectively. The proposed terrace-truncated nanocone structure of Al doped ZnO has suitable characteristics to use as a transparent conductive oxide material.

Zinc oxide is II-IV semiconductor material with unique properties such as direct wide band gap (3.37 eV), large exciting binding energy at room temperature (~60 meV), excellent thermal stability, splendid electron mobility and nontoxicity. [1-3)] It is widely used as a transparent conductive oxide material (TCO) in many industries such as solar cells, organic photovoltaics (OPVs) and display devices, sensors, liquid crystal displays (LCDs) and light emitting diodes (LEDs). In order to increase the electrical and optical properties, ZnO is doped with impurities. [4-11)] In general, ZnO is doped with Ga, Al, In, Tl, Co, Cu, Ag or Sn. Properties of impurity doped ZnO is vary with the dopant material. The dopant and the doping concentration highly decide the structure and characteristics of ZnO lattice. [12-17)] During the doping process, doping level should possess at relatively low level to avoid the lattice distortion, due to the difference of ionic radii of Zn and

impurity atoms. However, when Al or Ga used as a dopant with Zn, lattice distortions are minimized, even at higher doping concentrations, due to their compatibility of ionic and covalent radii with native Zn atoms. [1, 18, 19)] There are many reports about formation of various kind of ZnO nanostructures such as, rods, plates, bridges, cones, nanotubes etc. 1-D nanorod structure is suitable for photovoltaic applications due to its high surface-volume ratio. [20-24)] However, some researches have been reported about usage of ZnO nanocone structure, which could be increase the light transparency by reducing the scattering. [25-26)] In this research we investigate about the transparent conductive oxide properties of terrace-truncated nanocone structure of Al doped ZnO by advanced spray pyrolysis method. To the best of our knowledge, there was no proper study was done under this research title. We have prepared 0.5 moldm^{-3} of Zn^{2+} solution by dissolving Zinc acetate dihydrate (Wako Pure Chemicals) in 400 ml of 2-methoxyethanol (Wako Pure chemicals). 15 drops of ethanolamine (Sigma Aldrich) was added as a stabilizer while stirring. Aluminum Nitrate Nonahydrate (Wako Pure Chemicals) was added for doping (Al:Zn = 2: 98). The solution was stirred for 60 minutes at 70 °C and aged for 24 hours at room temperature.

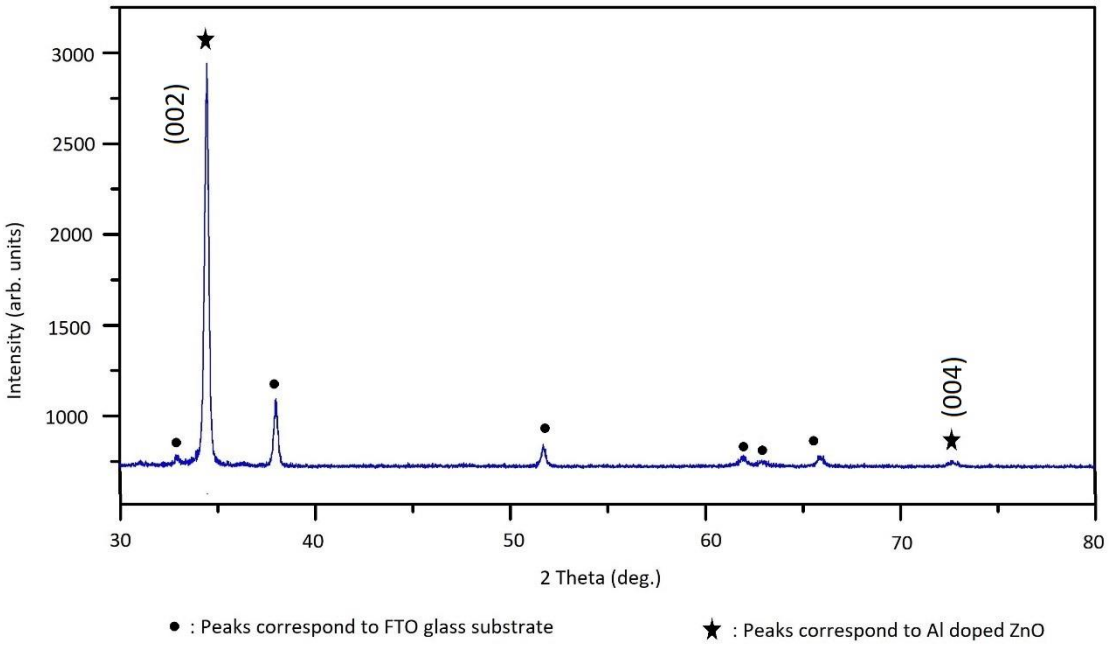

Fig.1. XRD patterns of Al doped ZnO Structure.

Commercially available FTO glasses (2.5 cm × 2.5 cm) were ultrasonically cleaned in a mixture of acetone, ethyl alcohol, and distilled water. Thickness of the FTO layer was 500 nm. Finally, precursor solution was deposited by using advanced spray pyrolysis deposition technique of rotational, pulsed and atomized (see supplementary data-fig.6). The deposition temperature, distance between nozzle tip and the glass substrate, spraying angle was kept constant at 400 ºC, 0.5 cm and 15°, respectively. Spray pressure was set to 0.40 MPa. Spraying was continued for 2 s, after 12 s of interval. Total spray time was 5.3 hours. Similar structural, optical and electrical results were obtained all over the glass substrate as we have used rotational spray pyrolysis deposition technique. Fig. 1 shows the XRD patterns of Al doped ZnO structure. Significant peak around 34.37º, shows the growth of nanostructure was favored in (002) direction of hexagonal wurtzite ZnO phase (JCPDS card No. 36-1451), which is along the c-axis, perpendicular to the FTO glass substrate. Weak peak around 72.5° is correspond to the (004) plane of ZnO, which is the replica peak of (002) plane of ZnO. [27)] All other peaks are corresponding for FTO layer.

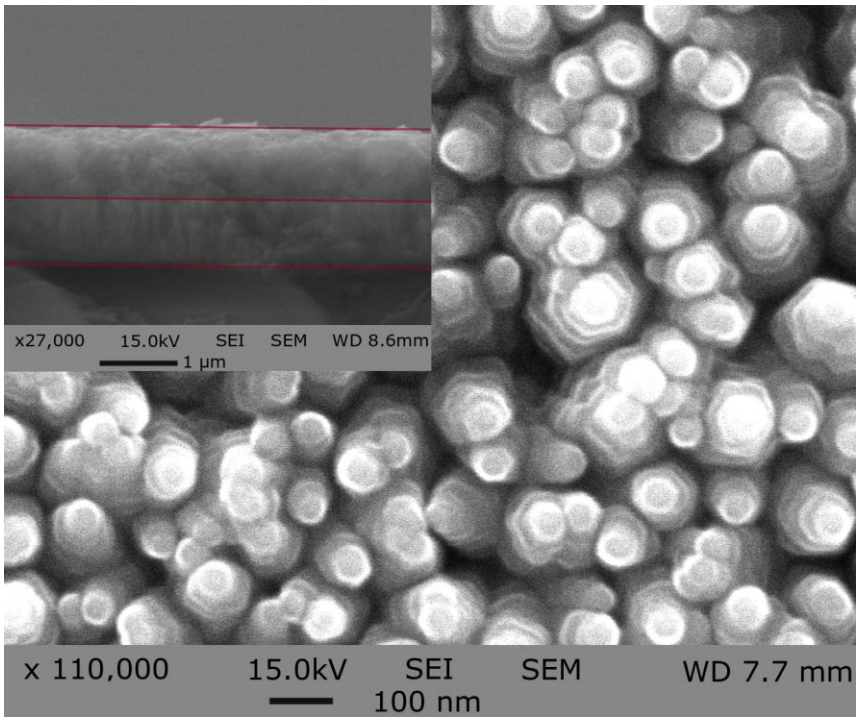

Fig.2. FE-SEM images of Al doped ZnO Structure.

Fig. 2 shows the FE-SEM images of Al doped ZnO nanostructure. Terrace-truncated nanocone structure could be confirmed by SEM images. The average top diameter and

the height of the nanostructure is 35-40 and 600-650 nm. We have confirmed the Al doping by EDX studies (see supplementary data-fig.7). The simulated terrace-truncated nanocone structure is shown in fig. 3, which was developed as a result of high growth rate along the (002) direction. In our deposition method, the total spray time was 5.3 hours. However, among this total spray time, 4.5 hours are spraying intervals. The spraying was continued only for 45 minutes. As the structure was grown along the c-axis by high growth rate, the decay rate is also high along the same direction. As a result, the hexagonal nanorod structure was end up as terrace truncated nanocone structure which was illustrated in fig.4. However, the bottom of the crystal structure was wide even though the top is decaying. This phenomenon might be occurred due to two main reasons which are,

- Decay rate along $(00\bar{2})$ direction of ZnO crystal structure is slow, as the growth rate along that direction is also slow.
- The bottom face of ZnO crystal structure (polar O^{2-} face) is tightly attached to the nucleation sites of the FTO glass substrate, which disturbs the decaying.

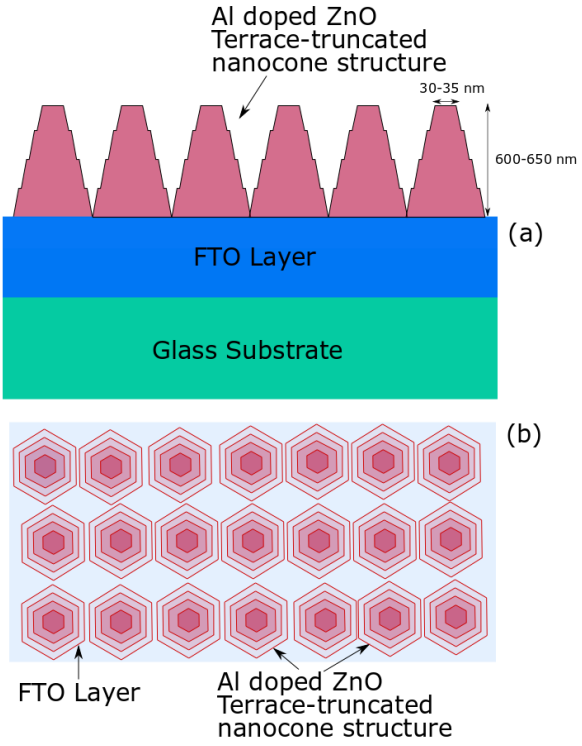

Fig.3. Simulated terrace-truncated nanocone structure of Al doped ZnO, (a). Cross section (b). Top view.

Rouhi et al also reported, the growth of nanocone structure is due to high growth rate of (002) plane with respect to non-polar surfaces, which leads to easy decay of (002) plane and end up with nanocone structure. [28,29)]

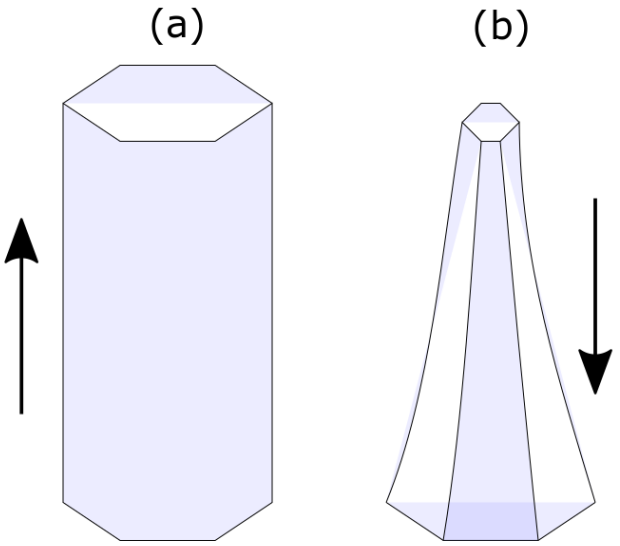

Fig.4. (a). Growth direction, (b). Decay direction of Al doped ZnO crystal structure.

There was no relationship was found in between ZnO nanocone structure and Al dopant as few reports were found about synthesize of pure ZnO nanocone structures. Rouhi et al reported about synthesizing ZnO nanocone structures. [28)] Visser et al also reported about the synthesize of ZnO nanocone structure. [30)] Fig. 5 shows the UV-visible spectrum of Al doped ZnO structure which confirms the average optical transmittance in the visible range was around 80%. Due to the terrace-truncated nanocone structure light harvesting is optimized as it has excellent antireflection properties. [28,31)] Moreover, narrow top of the synthesized structure helps to increase the light transparency by decreasing the light scattering. (see fig.8 of supplementary data). In general, 80- 93% of optical transparency could be obtained by Al based ZnO based TCO substrates. [32-34)] However, the optical transmittance of our structure was not as high as we expected, due to the light scattering at the boundary in two layered structure (FTO layer and Al doped ZnO layer). But the obtained optical transparency was in the transmittance range of a typical transparent conductive material, which is ~ 80%.

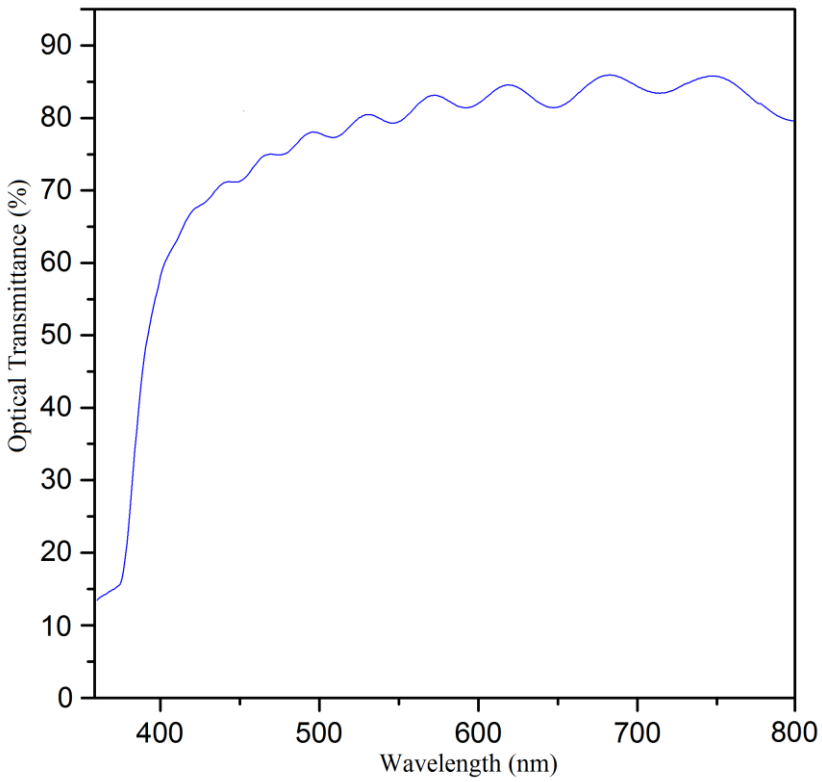

Fig.5. UV- visible spectrum of Al doped ZnO crystal structure.

Electrical studies of terrace-truncated nanocone structure of Al doped ZnO were done by using four probe method. Al doped ZnO is n-type conductive material due to oxygen and interstitial Zn defects. Sheet resistance, resistivity, mobility and conductivity were 4.87 $\Omega.sq^{-1}$, 1.9×10^{-4} Ω. cm, 10.63 $cm^2.V^{-1}.S^{-1}$ and 5.1×10^3 $\Omega^{-1}.cm^{-1}$, respectively. In this study we have deposited Al doped ZnO nanostructure on top of FTO glass substrate to increase the electrical conductivity. Sheet resistance was decreased by incorporating Al doped ZnO nanocone structure on FTO glass substrate, as sheet resistance of bare FTO glass substrate was <8 $\Omega.sq^{-1}$. Gondoni et al reported the resistivity of Al:ZnO nanostructure was 4.5×10^{-4} Ω. cm. [32] Mohammad et al reported, electrical conductivity of Al doped ZnO was 0.3 $\Omega^{-1}.cm^{-1}$. [34] The electrical conductivity obtained by our structure was high, with respect to other Al doped ZnO based structures. We investigate the growth mechanism and properties of terrace-truncated nanocone structure of Al doped ZnO, which was synthesized by using advanced spray pyrolysis deposition technique. Average top diameter was 30-35 nm and the heights are varying around 600-650 nm. XRD patterns confirms the vertical growth of the structure, which is perpendicular to the FTO glass substrate. This structure was obtained as a result of high growth rate which leads to high decay rate in a certain direction. The synthesized terrace-truncated nanocone

structure has excellent transparent conductive oxide properties of 80 % optical transmittance at the visible range and $5.1 \times 10^3\ \Omega^{-1}.cm^{-1}$ of electrical conductivity.

References

1. D.C. Look, Mat. Sci. Eng. B **80**, 383 (2001).
2. P. Ynag, H. Yan, S. Mao, R. Russo, J. Johnson, S. Richard, N. Morris, J. Pham, R. He, and H.J. Choi, Adv. Func. Mater. **12**, 323 (2002).
3. B. Ismail, M. Abaab, and B. Rezig, Thin Solid Films 383, **92** (2001).
4. G. H. Lee, Y. Yamamoto, M. Kourogi, and M. Ohtsu, Thin Solid Films **386**, 117 (2001).
5. P. F. Carcia, R. S. McLean, M. H. Reilly, and G. Nunes Jr., Appl. Phys. Lett. **82**, 1117 (2003).
6. J. Y. Chen and K. W. Sun, Sol. Energy Mater Sol. Cells **94**, 930 (2010).
7. C. S. Rout, A. R. Raju, A. Govindaraj, and C. N. R. Rao, Solid State Commun. **138**, 136 (2006).
8. K. Park, Deok-Kyou Lee, Byung-Sung Kim, Haseok Jeon, Nae-Eung Lee, Dongmok Whang, Hoo-Jeong Lee, Youn Jea Kim, and Jong-Hyun Ahn, Adv. Funct. Mater. **20**, 3577 (2010).
9. T. Prasada Rao, M.C. Santhosh Kumar, J ALLOY COMPD. **506,** 788 (2010).
10. Chih-Hsiung Hsu and Dong-Hwang Chen, Nanotechnology **21**, 285603 (2010).
11. Erki Kärber, Taavi Raadik, Tatjana Dedova, Jüri Krustok, Arvo Mere, Valdek Mikli, Malle Krunks, Nanoscale Res. Lett. **6,** 359 (2011).
12. S.J. pearton, D.P. Norton, K. Ip, Y.W. Heo, and T. Steiner, Prog. Mater. Sci. **50**, 293 (2005).
13. K. H. Kim, Z. Jin, Y. Abe, and M. Kawamura, Superlattices Microstruct.**75**, 455 (2014).

14. Shahzad Salam, Mohammad Islam, and Aftab Akram, Thin Solid Films **529**, (2013) 242.
15. J.W. Chen, D.C. Perng, and J.F. Fang, Sol. Energy Mater. Sol. Cells **95**, 2471 (2011).
16. J. Zhang, W. Que, F. Shen, and Y. Liao, Sol. Energy Mater. Sol. Cells **103**, 30 (2012).
17. S.H. Lee, S.H. Han, H.S. Jung, H. Shin, J. Lee, J.H. Noh, S. Lee, I.S. Cho, J.K. Lee, J. Kim, and H. Shin, J. Phys. Chem. C **114**, 7185 (2010).
18. F.Z. Bediaa, A. Bedia, M. Aillerie, N. Maloufi, F. Genty, B. Benyoucef, Energy procedia **50**, 853 (2014).
19. H. Quang Le, z Swee Kuan Lim, G. Kia Liang Goh, Soo Jin Chua, and JunXiong Ong, J. Electrochem. Soc.**157** [8], H796 (2010).
20. J. Song, S. Lim, J. Phys. Chem. C **111**: 596 (2007).
21. Y. Xia, P. Yang, Y. Sun, Y. Wu, B. Mayers, B. Gates, Y. Yin, F. Kim, and H. Yan, Adv. Mater. **15**, 353 (2003).
22. M. W. Chen, C. Y. Chen, D. H. Lien, Y. Ding, and J. H. He, Optics Exp. **18**, 14836 (2010).
23. S. Bai, W. Wu, Y. Qin, N. Cui, D. J. Bayerl, and X. Wang, Adv. Funct. Mater. **21**, 4464 (2011).
24. N. Alvi, K. ul Hasan, O. Nur, and M. Willander, Nanoscale Res. Lett. **6**, 130 (2011).
25. Z. Yin, X. Liu, Y. Wu, X. Hao, and X. Xu, Opt. Express. **20** [2], 1013 (2012).
26. J. Zhu, Z. Yu, G.F. Burkhard, C.M. Hsu, S.T. Connor, Y. Xu, Q. Wang, M. McGehee, S. Fan, and Y. Cui, Nano Lett. **9** [1], 279 (2009).
27. H. Liu, S. Gao, F. Zeng, C. Song and F. Pan, Phys. Status Solidi RRL **7**, 587 (2013).
28. J.Rouhi, M. H. Mamat, C. H. Raymond Ooi, S. Mahmud, and M. R. Mahmood, PLoS One. **10** [4], e0123433 (2015).

29. J. Rouhi, M. Alimanesh, R. Dalvand, C.H. R. Ooi, S. Mahmud, and M. R. Mahmood, Ceram. Int. **40**, 11193 (2014).
30. D. Visser, Z. Ye, C. S. Prajapati, N. Bhat, and S. Anand, ECS J. Solid State Sci. Technol. **6** [9], 653 (2017).
31. R. Pawar, J. Shaikh, P. Shinde, and P. Patil, Materials Letters **65**, 2235 (2011).
32. P. Gondoni, M. Ghidelli, F. Di Fonzo, V. Russo, P. Bruno, J. Martí-Rujas, C.E. Bottani, A. Li Bassi, and C.S. Casari, Thin Solid Films. **520**, 4707 2012.
33. M. Caglar, S. Ilican, Y. Caglar, and F. Yakuphanoglu, Appl Surf Sci. **255** 4491 (2009).
34. M.T. Mohammad, A.A. Hashim, and M.H. Al-Maamory, Mater. Chem. Phys. **99**, 382 (2006).